Available online at www.eccomasproceedia.org
Eccomas Proceedia COMPDYN (2025) 973-985

ECCOMAS
Proceedia

COMPDYN 2025
10th ECCOMAS Thematic Conference on
Computational Methods in Structural Dynamics and Earthquake Engineering
M. Papadrakakis, M. Fragiadakis (eds.)
Rhodes Island, Greece, 15-18 June 2025

MODELLING THE COLLAPSE OF A MASONRY TOWER DURING THE 2015 NEPAL EARTHQUAKE WITH SUPPORT FROM A VIDEO-CAMERA RECORDING

José V. Lemos[1], **Carlos Sousa Oliveira**[2], **and Rajesh Rupakhety**[3]

[1] National Laboratory for Civil Engineering (LNEC), Lisbon, Portugal, vlemos@lnec.pt

[2] Civil Engineering, CERis/IST, University of Lisbon, Lisbon, Portugal, csoliv@civil.ist.utl.pt

[3] Faculty of Civil and Environmental Engineering, University of Iceland, Selfoss, Iceland, rajesh@hi.is

Abstract

During the April 25, 2015 Nepal earthquake, the Dharahara Tower, a 60 m high historical brick masonry structure, located in Kathmandu collapsed completely. The tower was initially built in 1832, having suffered a previous failure at mid-height in 1934. The 2015 collapse event was previously analyzed by various authors using numerical models, focusing on the likelihood of a bending failure, as it had happened during the 1934 earthquake. However, a video camera recording recently found is not consistent with this mode of failure, as it shows the top of the tower descending vertically more than 10 m, before the initiation of overturning. In the present paper, a discrete element model is used to analyze the potential collapse modes. The model, based on the mechanical properties obtained in experiments on similar local building materials, was subject to the seismic records measured in the accelerometric station closest to the site. The new numerical model shows that a different type of mechanism is possible, triggered by compressive failure at the base and progressing by shearing along an inclined plane through the lower part of the structure. The results are consistent with the video images and also with the geometry of the tower segment remaining at the site. Parametric analyses were performed to investigate the role of a long period pulse present in the seismic records on the observed damage and collapse.

Keywords: Masonry tower, Nepal earthquake, Discrete element method, Back-analysis, Video monitoring.

ISSN:2623-3347
Peer-review under responsibility of the organizing committee of COMPDYN 2025.
doi: 10.7712/120125.12463.24541

1 INTRODUCTION

The 2015 Nepal earthquake caused a large number of human casualties and extensive damage including the collapse of many historical structures and monuments [1, 2]. Images and movies have documented the consequences of the event in various locations in Kathmandu [3]. The performance of structures of different types during the seismic event has been analysed by means of numerical models [4, 5]. The dynamic response of historical masonry towers and slender structures has been approached by finite element models [6, 7], as well as discrete element models (DEM), based on discontinuum representations [8, 9].

The present investigation is focused on the failure of the Dharahara Tower during the 2015 event [10]. This structure, built in 1832, has suffered damage and undergone several reconstructions, namely after the 1934 earthquake, when it broke at mid-height. A recently found video recording provides images of the early stages of collapse of the structure [3], showing that the top of tower started to move vertically downwards by several meters before falling sideways. Prior studies of the Dharahara tower using a discrete element model [11], or rocking dynamics [12], focused on collapse mechanisms similar to the one observed in 1934, ensuing from the cracking of bricks at mid height and followed by overturning of the upper part. However, the recently found video evidence is not consistent with this more common type of bending failure. The analysis of the remains of the tower show a "triangular" section still standing suggesting the accident may have been triggered by a shear failure plane near the base of the structure. A new discrete element model was developed to investigate this alternative collapse mode, applying as dynamic input the motion recorded in a seismological station nearby, and using for comparison the video recording of the movement of the upper section of the tower. If the shear plane failure is not considered, the present model provides solutions similar to the previous studies [11].

2 THE 2015 NEPAL EARTHQUAKE

The Mw7.8 Gorkha earthquake of 25 April 2015 occurred on a segment of the Main Himalayan Thrust fault, a low-angle subduction interface between the Indian Plate and the Eurasian Plate [13]. The epicentre was located about 80km WNW of Kathmandu, with the rupture propagated towards the East, with a large part of slip occurring just North of Kathmandu [14]. The Dharahara Tower is located in the Kathmandu Valley. The valley contains deposits of upper Pliocene to Quaternary clay, silt, sand and gravel. More than 300m thick muddy and sandy lacustrine sediments overlay sand and gravel in most parts of the Valley.

Ground shaking during the mainshock was recorded at several stations in the Valley, and the motion records at different stations have been compared [14, 15]. A striking feature of ground motion recorded in the valley is a large amplitude pulse with a period of approximately 5s, which has been attributed to source radiation and local site effects including generation of Love type surface waves [15]. The horizontal Peak Ground Acceleration varied from 0.13 to 0.26g, which is considered low for an earthquake of this size. This has been attributed to the filtering of high frequency waves by the sediments of the Valley. The station KTP, lying on a rock outcrop, recorded significantly lower energy (Arias Intensity) than stations in the Valley, despite higher PGA at this station. The higher energy in the softer sites has been shown to be mostly contributed by waves with period 5s [14].

The closest recording station to the Dharahara Tower is the KATNP at a distance of about 1.3 km [15]. Ground acceleration, velocity and displacement at this station are shown in Figure 1. The ground velocity in both horizontal and vertical directions is characterized by a strong one-sided pulse, which results in a permanent displacement offset of 73, 177, and 110 cm in the West, South, and Up directions, respectively.

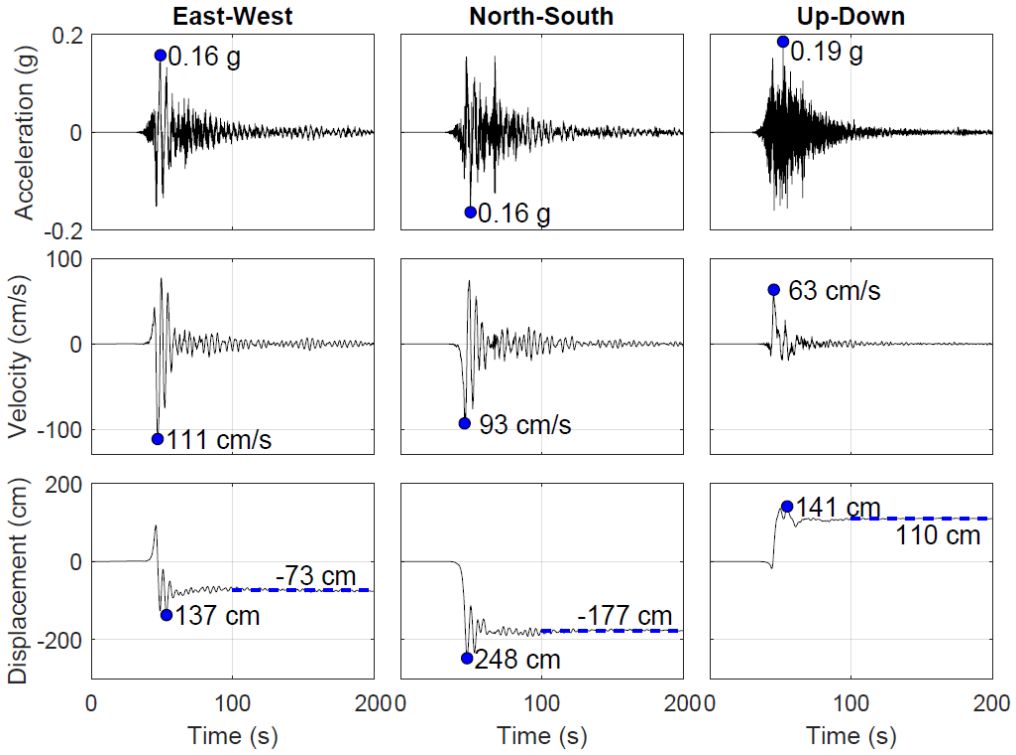

Figure 1. Ground acceleration, velocity, and displacement at the KATNP station [15].

Elastic pseudo-acceleration spectra of horizontal ground motion at KATNP is shown in Figure 3. A clear peak at a period of about 5s is clearly visible in the response spectra. The Fourier Amplitude Spectra of acceleration recorded at the rock site KTP contains a significant peak at a period of about 5s, indicating that the pulse is not entire due to basin and/or local site effects [15]. Nevertheless, the 5s peak is much larger at KATNP than at KTP, which indicates that the valley response amplified this pulse. The motion at KATNP is strongly polarized on the horizontal plane, implying that the 5s pulse is a result of source effect and surface Love waves generated and trapped in the valley. Another clear peak around 0.4s is dominant in the N-S direction. When the motion is projected on the principal directions [16], which is suitable for a symmetric structure like the Dharahara Tower, a clear peak appears at a period of about 2s, which is close to the fundamental vibration period of the tower. At this period, the motion seems highly anisotropic.

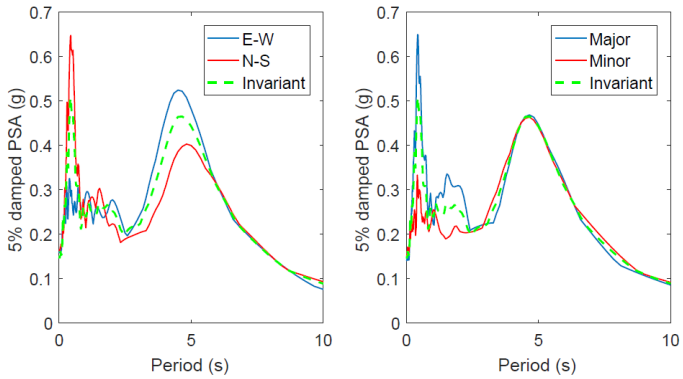

Figure 2. Elastic response spectra (5% damped) of horizontal motion at KATNP station. (left) Correlated motion in the EW and NS direction; (right) uncorrelated motion projected in the major and minor directions [16].

3 THE DHARAHARA TOWER

The Dharahara Tower, 61m high, is an almost cylindrical structure with a gradual reduction of wall thickness along the height (Figure 3). The core is cylindrical and the helicoidal stairway is supported by both the wall and the core, going up clockwise. The tower stands on a conical pulpit with 8 levels, which gives access to the entrance door. The exterior wall is divided into 7 sections bounded by cornices and several circular windows following the course of the stairs. There is a balcony near the top of the tower, ending in a dome with a bronze pinnacle. The doors, at the entrance and at the balcony, open to the East. The outer diameter is 6.38m at the bottom, and 3.43m at the top. The wall thickness ranges from 1.82m at the bottom, to 0.73m at the top. Typical brick size is 0.22x0.15x0.05m. Figure 4 shows the collapsed structure after the 2015 earthquake, and a detail of the brick wall.

Figure 3. The Dharahara Tower, view and vertical cross-section.

Material properties for structures of the same era as the Dharahara tower cover a wide range [17, 18, 19]. Compressive strengths of the bricks range from 4 MPa to 20 MPa. In some cases, the reported values of compressive strength for prism tests are quite low, in the order of 1 MPa. At the base of Dharahara tower, with its 60 m height, vertical stresses up to 1.5 MPa are estimated in the numerical model. Seismic events in the structure's lifetime must have induced higher stresses without apparent damage. Thus, the material strength is likely to be in the upper range of the values published in the literature. In the present study, the properties assumed for compressive strength are based on reference [11]. In the numerical model, the uniaxial compressive strengths were taken as: brick, 10 MPa; mortar, 1.4 MPa; and, wall, 2.0 MPa. The wall Young's modulus was taken as 3 GPa.

4 THE COLLAPSE

The collapse can be understood through images and video-camera footage. The post event images show many of the material features, the brick arrangement, the stairway, the entrance door, and the final disposition of all elements after impact on the ground (Figure 4). From the images, we see that the collapse was almost total with two essential features: the formation of an almost planar shearing surface at the first few meters of the tower at an angle of 65° with the horizontal. The remains of the tower below this plane remained intact. The tower seems to

have first slipped down this plane before overturning sideways in relation to the plane, disintegrating almost entirely into many pieces (bricks and brick walls segments). The plane dips Southeast with the lower tip near the entrance. The main debris rubble is located in the Southwest. The pulpit was destroyed in front of the sliding plane and several bulky volumes of bricks can be seen still forming cemented blocks.

Figure 4. (left) The remaining part of the tower after the 2015 earthquake; (right) detail of the brick wall.

The video camera recording [3], shot from the Southeast through a zone of trees and bushes, shows the collapse in its initial phase and the overturning of the tower (Figure 5). It does not show the crushing of the collapsed tower on the ground. This video, even though of poor quality, shows two important stages. The first is the vertical descent of several meters of the upper part of the shaft with a small translational movement to the Southwest; then, after an instantaneous stop, the shaft starts to overturn towards the back. The structure's shaft is divided vertically into 8 main segments, marked by peripheral salient rings, with an average height of about 6 m (Figure 2). The video shows that, in the initial stage of collapse, 3 of these segments move down almost vertically, before the overturning movement initiates (Figure 5).

The use of video images to support back-analysis of structures is becoming an important source of information, as more and more cameras are being installed. In the case of earthquakes, they may provide essential data to understand the behaviour of many structures during these events [20].

Figure 5. Video images of the collapse. a) b) Top of tower shaft moving down several meters and slightly westwards; c) overturning.

5 NUMERICAL MODELING OF THE TOWER COLLAPSE

5.1 Geometry and material properties

The discrete element model of the tower (Figure 6), was built with the code 3DEC [21], often applied in the analysis of masonry structures. The x-axis points in the East direction, where the entrance is located, while the y-axis points North. The model geometry was generated inside 3DEC, using the script language Fish. The model is based on a rigid block representation, the most common choice for dynamic analysis with discrete elements, as it is capable of simulating the discontinuous nature of the masonry material without excessive computational requirements. In a rigid block model, all the system deformation and non-elastic behaviour are lumped at the joints. Thus, the jointing pattern is required to encompass the expected modes of deformation and collapse. Failure through the blocks may be accounted for by cutting them with potential failure planes, which are assigned the strength of the intact material and will fail only if the stresses reach that level. Given the large size of the structure, the real dimensions of the individual bricks cannot be reproduced. The numerical model blocks are much larger than the real bricks, but the joint properties which govern the deformability of the rigid block system are calibrated to provide the intended global Young's modulus of the masonry material. Thus, zero-thickness interfaces represent the mortar joints, as done in finite element micro-models. The numerical block size should provide a sufficient number of joints to allow a variety of failure modes to develop through them. In the present case, given the need to investigate the potential nonlinear behaviour in the lower part of the tower, a more refined discretization was used there, reducing the joint spacing in the horizontal and radial directions (Figure 6). The joint stiffnesses of each region are properly calibrated to account for the different spacing, as described below. The block imbrication is given by creating macro-blocks formed by 2 adjoining rigid blocks, as shown in the detail of a wall segment (Figure 6).

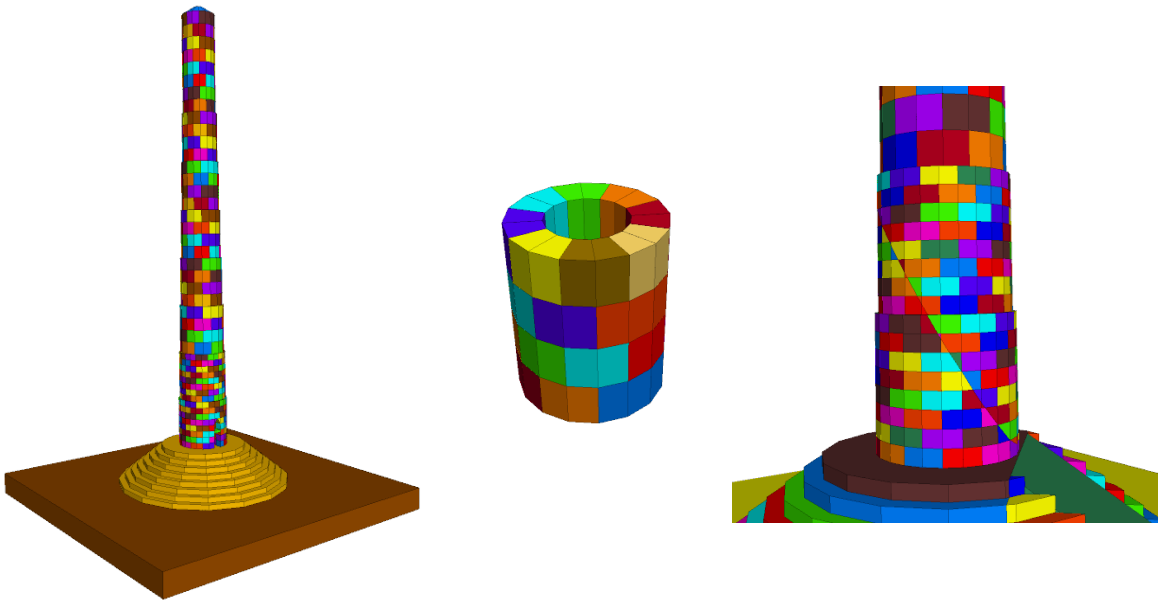

Figure 6. Discrete element model of Dharadara Tower. Global view; detail of the wall blocks; and, detail of the lower part with the potential shear failure plane.

The Young's modulus for brick assemblies was taken as E=3 GPa. The input elastic properties in a rigid block system are the joint stiffness parameters in the normal and shear directions. The joint normal stiffness was taken as E/s, where s is the average block dimension in the direction normal to the joint, in order to provide an average uniform deformability independent of the numerical block size. The joint shear stiffness was taken as half of the normal stiffness. The nonlinear behaviour of the joints was based on a Mohr-Coulomb constitutive model. For the horizontal joints, the strength properties were taken as those of mortar. Considering a uniaxial compressive strength of 1.4 MPa, the corresponding Mohr-Coulomb parameters were a friction angle of 30º and a cohesion of 0.40 MPa. The tensile strength of the joints was taken as 0.20 MPa, half of the cohesive strength. The vertical joints in the numerical model are through-going while in reality the brick imbrication implies that failure along these planes must cut through the brick material. Thus, the strength of the vertical joints was taken from the brick material, with a uniaxial compressive strength of 10 MPa, a friction angle of 30º and a cohesion of 2.88 MPa, and a tensile strength of 1.44 MPa. Table 1 summarizes the mechanical properties of the joints.

	Horizontal joints	Vertical joints	Inclined plane
Normal stiffness (MPa/m)	1940 (U) 3870 (L)	1900 (U) 2860 (L)	5000
Shear stiffness (MPa/m)	970 (U) 1935 (L)	950 (U) 1430 (L)	2500
Cohesion (MPa)	0.40	2.88	2.88
Tensile strength (MPa)	0.20	1.44	1.44
Friction angle (º)	30	30	30

Table 1. Joint mechanical properties (U: upper part; L: lower part)

Assuming elastic behaviour of all joints, it is possible to obtain the natural frequencies of the block system. The first bending mode, almost similar in the two orthogonal directions, has a frequency of 0.5 Hz. The frequency of the second bending modes is 2.0 Hz, while the third bending modes is 4.7 Hz. There is a torsional mode with frequency 4.6 Hz, and a vertical mode with a frequency of 6.8 Hz.

The simulation of the earthquake was conducted by a time domain nonlinear analyses. The code 3DEC employs an explicit algorithm, capable of representing the progressive changes in geometry, with the consequent update of the location of the contacts between the blocks, whenever a failure mode develops. Given the numerical stability requirement for this type of algorithm, very small time steps have to be used, in this case in the order of 1.0×10^{-5} s, which leads to large run times. Viscous damping was considered, based on the mass-proportional component of Rayleigh damping with 5% of critical at 0.5 Hz. Frictional sliding at the joints provides additional energy dissipation. The input motion was prescribed at the base block, in the 3 directions, using the records measured at the KATNP station (Figure 1).

5.2 Base model. Bending failure mode

As discussed, the tower was previously analyzed by another 3DEC model [11], showing a bending failure mode, with the upper part toppling above a hinge located roughly about mid-height. The present 3DEC model is more refined, using smaller block sizes, and different material properties values were assumed, based on the currently available experimental data sources. However, when the seismic records were applied, the failure mode was qualitatively

similar to the one obtained in the previous study, also involving bending and breakage of the tower about mid-height (Figure 7). As explained in the previous section, this failure mechanism does not fit the movement observed in the video, which shows the upper part of the tower going down vertically for a few meters.

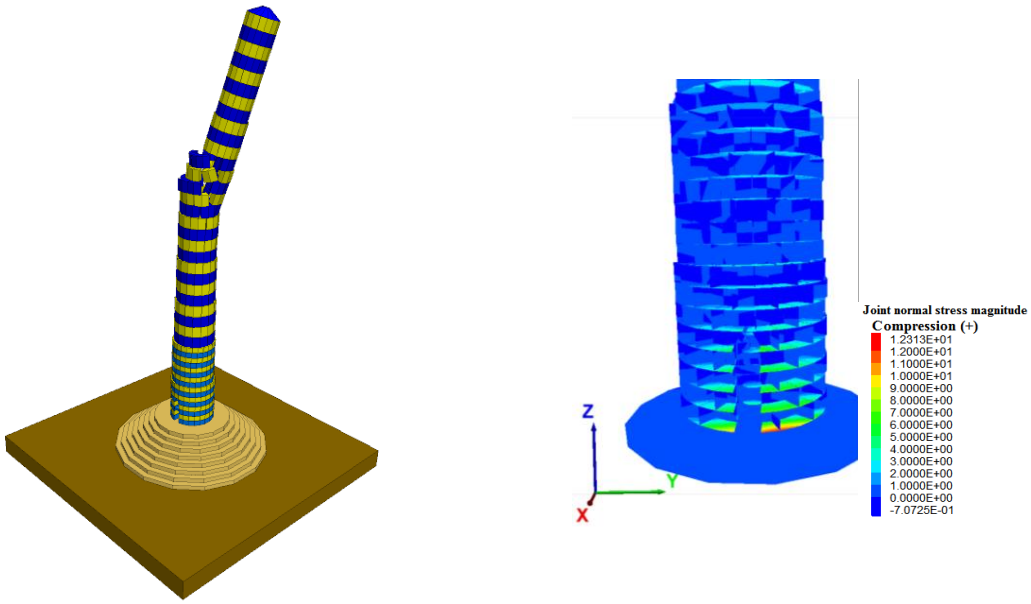

Figure 7. Base model, without considering the shear failure plane. (left) Collapse mode; (right) Vertical stresses at the base of the tower at t = 46 s (max. 12.3 MPa).

Inspecting the joint stresses which develop at the lower joints of the tower during the seismic event, we see that the vertical component exceeds the brick strength, as shown in Figure 7. At t=46 s we have a peak of 12 MPa and at t=47 s, it increases to 17 MPa. This suggests the possibility of compressive crushing or shear failure of the material near the base of the structure, which was investigated as explained in the next section. The orientation of the plane showing larger stresses dips downwards, passing through the door of the tower, emphasizing the role of that weak structural region in the overall behaviour of the tower.

5.3 Model considering the shear failure plane

The part of the structure which remained standing after the earthquake suggests that shear failure took place along an inclined plane reaching the base of the tower (see photo in Figure 4). When using rigid block models, failure through the blocks can be simulated using the "bonded-block model" approach [22]. In this type of model, rigid blocks are split into an assembly of smaller blocks bonded together. The bond strength is based on the intact material properties, and can be represented by the Mohr-Coulomb parameters cohesion, friction angle and tensile strength. The interfaces between the sub-blocks define the potential failure planes. If the stresses along these interfaces reach the strength envelope, the bonds break and the sub-blocks start to slide or move apart.

The discrete element base model was modified by introducing a potential shear failure plane in the lower part of the tower, according to the geometry of the remaining part (Figure 6). The properties of the contacts along the inclined plane were taken as the brick strength listed above (uniaxial compressive strength of 10 MPa; friction angle of 30º; cohesion of 2.88 MPa; tensile strength of 1.44 MPa). Failure on this plane only takes place if the stresses reach the failure envelope of the intact material.

The lower part of the model was simplified, replacing the steps by a sloping plane, reproducing what can be seen in the images of the post-collapse situation. The dynamic impact of the falling structure is difficult to simulate. Therefore, in the simplified model, this event is essentially governed by 2 parameters: the stiffness of the new contacts between the falling tower shaft blocks and the slope, taken as 194 MPa/m, in the normal direction, and half of this value in shear; and, the friction angle of 30º. The stiffness value is low, intending to simulate a relatively soft impact, as the structure is breaking into small pieces. There is no experimental support for these values, but they only influence the results in the final part of the collapse process.

During the dynamic analysis, at t=46.3 s, some contacts break at the bottom of the potential shear plane, consistent with the large vertical stresses in this region shown in Figure 7. This event follows immediately the peaks of 0.16 g in the applied acceleration record in the North-South and East-West directions (Figure 1), which are likely to produce high compressive stresses at this location. The failure quickly propagates upwards along the plane, so that at t=46.8 s, all the shear plane is sliding, already with movements of about half a meter.

The sequence of the structural collapse process is shown in Figure 8. At t=48.5 s, sliding of several meters along the shear failure plane brings the top of the tower vertically down, as seen in the video. The sliding continues, and at t=48.5-49 s the tower wall starts to disaggregate. Finally, at t=50 s, the tower overturns falling over the triangular portion. This final movement does not agree with the observed result, as in reality the tower moved further sideways, essentially to the left, and did not destroy the triangular part. This disagreement is understandable, as much simplified numerical models always have difficulty in reproducing the events after very large movements take place. Sliding down the shear plane, a rough surface involving brick breakage, as well as the impact on the lower steps of the pulpit, are complex phenomena which cannot be simulated accurately with the available data. Therefore, the final part of the numerical simulation may vary significantly if we change the geometric and mechanical properties of the model. This is typically the case for analyses involving very large displacements, where the outcome starts to depend on model details, e.g. how smooth is the sliding plane cutting through the bricks. In addition, the process of breakage of the walls, seen developing at t=49 s, also depends on how sharp is the impact of the sliding body on the ramp at the model base, which is governed by damping and base properties difficult to estimate. Moreover, we are using as input the ground motion recorded approximately 1.3 km away from the location of the Tower. Actual ground shaking at the site, especially in terms of their relative intensities and phases in the two horizontal directions is probably different from what was recorded at KATNP. Due to these uncertainties, it is not possible to simulate properly the final stages of the collapse process. However, the important observation that failure started along a shear plane along which the upper portion slid for a few meters before hitting the ground and toppling is accurately simulated by the numerical model.

Given the uncertainty about the material properties, another analysis was performed assuming the brick compressive strength to be 5.5 MPa [19], instead of 10 MPa. The initiation and early stages of the collapse mechanism are similar, with sliding on the inclined plane. As the sliding wall approaches the base, differences in the movement can be observed. The lower compressive strength leads to a faster disaggregation of the lower section of the wall, followed by a lateral overturning. The variability of the later stages of collapse is to be expected, as noted above. However, the essential features remain unchanged.

In order to estimate the safety margin of the structure, parametric studies were performed in which the input record was scaled by factors ranging from 0.5 to 0.9. For factors of 0.8 and 0.9, the same collapse mechanism occurred. For a scaling factor of 0.7, corresponding to acceleration peaks in order of 0.11g, no collapse took place. There was no failure on the inclined

surface, but shearing on a horizontal joint at about mid-height led to a permanent displacement of 0.4 m at this joint. For 0.6 of input and lower, the structure survived with almost no damage.

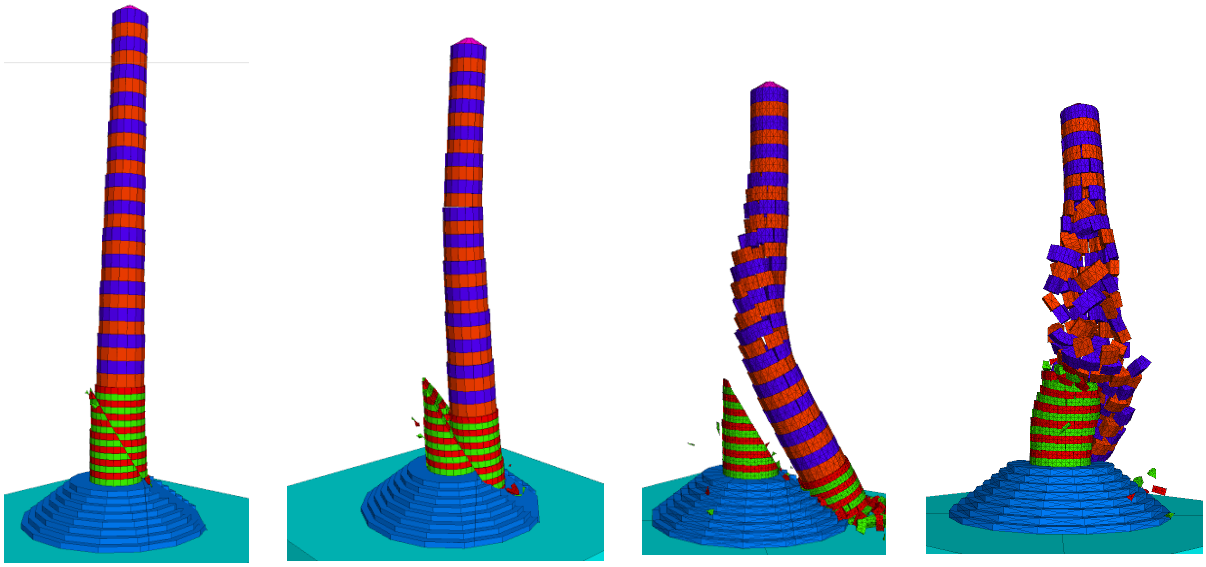

Figure 8. Numerical simulation of collapse: (a) t=47 s, (b) t= 48 s; (c) t =49 s; (d) t =50 s, view from NW.

In order to study the effects of the 5 s pulse (Figure 2) on the structural response, a further set of analyses was performed with modified input records, in which a band pass filter 0.3-25 Hz was applied to remove the pulse. These simulations did not lead to collapse. A scaling factor of 1.7 had to be applied to trigger the shear failure along an inclined plane and cause collapse. In this case, the inclined plane would dip in the opposite direction, and the failure was initiated at t=50s, when the acceleration peaks caused the higher stressing, this time at the opposite point of the tower base. These results indicate the significant importance of the low frequency pulse deriving from the local conditions of the valley.

6 DISCUSSION AND CONCLUSIONS

A study of the collapse of Dharahara Tower, in Kathmandu, during the 2015 Nepal earthquake, partially observed in a video camera footage, was conducted by means of a numerical model. The following conclusions can be taken:

- The discrete element model reproduced quite fairly the main features of the observed collapse mode of the tower. The model is based on a simple mechanical representation using rigid blocks and frictional joints, therefore involving a relatively small number of input parameters.
- This modelling approach provides the dynamic evolution of the structure from the initial stage to the complete collapse. Many simplifying assumptions are required due to the shortage of experimental information and the computational limitations, so parametric studies are important to evaluate their effects. In particular, the advanced stages of the collapse process can never be fully predicted as they depend on many details.
- Even considering the significant uncertainties, namely regarding the ground motion and the mechanical properties, it is possible to say that the model results are consistent with the recorded video cameras and the post-collapse information.

- The low frequency pulse present in the input records, reflecting the local conditions in the valley, was found to have a significant effect on the structural response of the tower.
- The importance of video images to understand the structural failure was critical in this case, as without the recorded images of the collapse initiation it would be impossible to reproduce the events.

7 ACKNOWLEDGEMENTS

We thank Arjun Shrestha, Akanksha Kunwar, and Pushpa Mahat for arranging visits to the site and collecting important data such as measurements of different parts of the remains of the Dharahara Tower. We also thank Dipendra Gautam for his input on selection of appropriate material properties.

REFERENCES

[1] K. Goda, T. Kiyota, R.M. Pokhrel, G. Chiaro, T. Katagiri, K. Sharma, S. Wilkinson, The 2015 Gorkha Nepal earthquake: insights from earthquake damage survey. *Frontiers Built Environment*, **1**, 1-13, 2015.

[2] S. Bhagat, H.A.D. Samith Buddika, R.K. Adhikari, A. Shrestha, S. Bajracharya, R. Joshi, J. Singh, R. Maharjan, A.C. Wijeyewickrema, Damage to Cultural Heritage Structures and Buildings Due to the 2015 Nepal Gorkha Earthquake. *Journal of Earthquake Engineering*, **22**, 1861-1880, 2018.

[3] YouTube, Dharahara Falling Live Nepal Earthquake 2072/2015, Kalo Biralo, 2015. Accessed October 3, 2023. https://www.youtube.com/watch?v=Qwr3bIjnzPo.

[4] R.K. Adhikari, D. D'Ayala, 2015 Nepal earthquake: seismic performance and post-earthquake reconstruction of stone in mud mortar masonry buildings. *Bulletin of Earthquake Engineering*, 18, 3863-3896, 2020.

[5] C.S. Oliveira, J.V. Lemos, Back-analysis of the Collapse of a Tetrastyle Canopy during the April 25, 2015 Nepal Earthquake. *International Journal of Architectural Heritage*, **17**, 418-430, 2021.

[6] F. Pena, P.B. Lourenço, N. Mendes, D. Oliveira, Numerical models for the seismic assessment of an old masonry tower. Engineering Structures, **32**, 1466-1478, 2010.

[7] M. Valente, G. Milani, Non-linear dynamic and static analyses on eight historical masonry towers in the North-East of Italy. *Engineering Structures,* **114**, 241-270. 2016.

[8] V. Sarhosis, G. Milani, A. Formisano, F. Fabbrocino, Evaluation of different approaches for the estimation of the seismic vulnerability of masonry towers. *Bulletin of Earthquake Engineering*, **16**, 511-1545, 2018.

[9] D. Malomo, B. Pulatsu, Discontinuum models for the structural and seismic assessment of unreinforced masonry structures: a critical appraisal. *Structures*, **62**, 106108, 2024.

[10] J.V. Lemos, C.S. Oliveira, R. Rupakhety, Collapse of the Dharahara Tower during the April 25, 2015 Nepal earthquake: A new interpretation based on video-camera footage. *International Journal of Architectural Heritage*, DOI:10.1080/15583058.2024.2385964, 2024.

[11] A. Mehrotra, M.J. DeJong, The Performance of Slender Monuments During the 2015 Gorkha, Nepal, Earthquake. *Earthquake Spectra*, **33**, S321-S343, 2017.

[12] A. Mehrotra, M.J. DeJong, The influence of interface geometry, stiffness, and crushing on the dynamic response of masonry collapse mechanisms. *Earthquake Engineering and Structural Dynamics*, **47**, 2661–2681, 2018.

[13] R. Bilham, Himalayan earthquakes: a review of historical seismicity and early 21st century slip potential. P.J. Treloar, M.P. Searle eds. *Himalayan Tectonics: A Modern Synthesis,* Geological Society, Special Publications, London, 483, 423-482, 2019.

[14] R. Rupakhety, Seismotectonic and Engineering Seismological Aspects of the Mw 7.8 Gorkha, Nepal, Earthquake. D. Gautam, H. Rodrigues, eds. *Impacts and Insights of the Gorkha Earthquake*, Elsevier, 2018.

[15] R. Rupakhety, S. Olafsson, B. Halldorsson, The 2015 Mw 7.8 Gorkha Earthquake in Nepal and its aftershocks: Analysis of strong ground motion. *Bulletin of Earthquake Engineering*, **15**, 2587-2616, 2017.

[16] R. Rupakhety, R. Sigbjörnsson, Rotation-invariant measures of earthquake response spectra. *Bulletin of Earthquake Engineering*, **11**, 1885-1893, 2013.

[17] H.R., Parajuli, J. Kiyono, H. Taniguchi, Structural assessment of the Kathmandu world heritage buildings. *Proceedings of the 31st Conference on Earthquake Engineering*, JSCE, 2011.

[18] R. Adhikari, P. Jha, D. Gautam, G. Fabbrocino, Seismic Strengthening of the Bagh Durbar Heritage Building in Kathmandu Following the Gorkha Earthquake Sequence. *Buildings*, **9**, 128, 2019.

[19] D. Gautam, R. Adhikari, S. Olafsson, R. Rupakhety, Damage description, material characterization, retrofitting, and dynamic identification of a complex neoclassical monument affected by the 2015 Gorkha Earthquake. *Journal of Building Engineering* **80**, 108152, 2023.

[20] C.S. Oliveira, M.A. Ferreira, Following the Video Surveillance and Personal Video Cameras: new tools and innovations to health monitor the earthquake wave field. *International Journal of Disaster and Risk Reduction*, **64**, 102489, 2021.

[21] Itasca, *3DEC - Three-dimensional distinct element code: Theory and background*, Version 5.2. Minneapolis, MN, USA: Itasca Consulting Group, 2018.

[22] V. Sarhosis, J.V. Lemos, A detailed micro-modelling approach for the structural analysis of masonry assemblages. *Computers and Structures*, **206**, 66-81, 2018.